

# Compartmental Analysis Suggests Macropinocytosis at the Onset of Diatom Valve Formation

H. J. Brasser · H. J. van der Strate · W. W. C. Gieskes · G. C. Krijger · E. G. Vrieling · H. T. Wolterbeek

Received: 21 April 2010 / Accepted: 5 October 2010  
© The Author(s) 2010. This article is published with open access at Springerlink.com

**Abstract** During valve formation of the siliceous frustules of diatoms, bulk uptake of silicic acid and its subsequent transport through the cell is required before it can be deposited in the silica deposition vesicle (SDV). It has been assumed that transport takes place via silicon transporters (SITs), but if that were the case a control mechanism would have to exist for stabilization of the large amounts of reactive silicon species during their passage through the cell on the way to the SDV. There is, however, no reason to assume that classical silica chemistry does not apply at elevated levels of silicic acid, and therefore autopolymerization could reasonably be expected to occur. In order to find alternative ways of Si transport that correspond with the high speed of valve formation at the earliest stages of cell division we followed  $^{31}\text{Si}(\text{OH})_4$  uptake in synchro-

nously dividing cells of the diatoms *Coscinodiscus wailesii*, *Navicula pelliculosa*, *N. salinarum*, and *Pleurosira laevis*. The results were related to systematically derived mathematical models for a compartmental analysis of 5 possible uptake/transport pathways, including one involving SITs and one involving (macro)pinocytosis-mediated uptake from the extracellular environment. Our study indicates that the uptake of radioactive silicic acid matches best with the model that describes macropinocytosis-mediated silicon uptake. This process is well in line with the observed ‘surge uptake’ at the start of valve formation when the demand for silicon is high; it infers that in diatoms a pathway of uptake and transport exists in which SITs are not involved.

**Keywords** Compartmental analysis · Diatoms · Si-31 · Valve formation · Silicon uptake

**Electronic supplementary material** The online version of this article (doi:10.1007/s12633-010-9059-2) contains supplementary material, which is available to authorized users.

H. J. Brasser · G. C. Krijger · H. T. Wolterbeek (✉)  
Faculty of Applied Sciences, Department of Radiation,  
Radionuclides & Reactors, Section Radiation and Isotopes for  
Health, Delft University of Technology,  
Mekelweg 15,  
2629 JB Delft, The Netherlands  
e-mail: h.t.wolterbeek@tudelft.nl

H. J. van der Strate · W. W. C. Gieskes  
Department of Ocean Ecosystems, Energy and Sustainability  
Research Institute Groningen, University of Groningen,  
PO Box 14, 9750 AA Haren, The Netherlands

E. G. Vrieling (✉)  
Groningen Biomolecular Sciences and Biotechnology Institute,  
University of Groningen,  
PO Box 14, 9750 AA Haren, The Netherlands  
e-mail: e.g.vrieling@rug.nl

## 1 Introduction

Diatoms (Bacillariophyceae) are unicellular eukaryotic photosynthesizing microalgae that often dominate the microalgal communities of marine and freshwater habitats. The most distinctive feature of diatoms is their frustule, an exoskeleton of amorphous silica that surrounds the cell [1, 2]. Silicon is necessary for frustule formation [1, 3] but it also acts as an essential trace element in other cellular compartments [4, 5]. The silicon required for the formation of the frustule has to be taken up by the cell and transported to the cellular compartment in which the siliceous parts of the frustule are formed: the SDV [1]. Silica formation in diatoms integrates silica chemistry, silicic acid polymerization and condensation [4, 6, 7] on the one hand and molecular pathways on the other [8, 9]. Much attention has so far been paid to the uptake of silicon by cells and

subsequent transport inside the cells (extensively outlined in Thamtrakoln & Hildebrand 2008 [10] and Hildebrand 2008 [11]). It has been proposed that the uptake is controlled by two mechanisms: uptake at lower silicic acid concentrations mediated by silicon transporters (SITs) and a diffusion-mediated route at higher silicon concentrations [10, 11]. Diffusion of Si, however, has not been demonstrated in diatoms; it has been correlated to data obtained on rat liver mitochondria [12]. Recent studies on yeasts showed that diffusion of Si in particular occurs when the integrity of membranes is at stake [13]. As such a diffusion mechanism for massive uptake of silicon in diatoms is questionable.

Silicic acid polymerizes to condensed silica when concentrations exceed 2 mmol/L [14, 15]. The polymerization reaction and physico-chemical properties of the solid silica are affected by the addition of surfactants (e.g. organic molecules, temperature, pH, and ionic strength [14, 15]). Based on *in vitro* studies it has been proposed that peptides like silaffins reduce the energy barrier for Si polymerization which could result in a lower threshold concentration for Si [11]. A decreasing pH in the SDV upon diatom valve maturation suggests enhancement of the finalization of the silica polymerization reaction [6]. Ionic strength determines the degree of condensation of the silica and affects the nanostructure of the solid silica formed in diatoms [7]. Noteworthy is that in diatoms early valve formation coincides with nanostructuring of the primer two-dimensional silica base [16, 17]. The impact of reaction conditions on silica polymerization in diatom frustule formation suggests that cellular transport routes during which polymerization of accumulated silicon species could occur are not likely to be involved in valve formation [4, 7]. Silicon in diatom cells (excluding the silica of the frustule) has been proposed to be present in a precondensed silica sol-like form [18], while during valve formation organo-silicon interactions occur [19]. The exact localization of these silicon species and their accumulation outside the SDV is under debate; distinct intracellularly confined silicon pools have never been detected [17, 20, 21], except the one in the SDV and the random distribution of very low silicon levels inside various cellular compartments [4, 5, 20, 21]. Thus, the absence of distinctive larger intracellular silicon pools is certainly not in line with an expected high uptake and intracellular transport of silicon required for valve formation.

The ionic strength of the surrounding medium has a strong influence on the biosilica nanostructure which may be explained by the influence of the salt concentration on the Si polymerization chemistry inside the SDV. To explain a direct influence an alternative silicon uptake pathway by (macro)pinocytosis has been proposed [7]. It remains to be shown whether or not this process takes place by: 1) ‘classical’ pinocytosis in which multiple smaller vesicles

are involved, or 2) macropinocytosis in which one larger vesicle is formed which transforms to become the initial SDV. The macropinocytosis hypothesis is supported by recent 3-D ultrastructural studies on SDV transformations [16] in which actin filaments are specifically involved in molding and/or compressing the SDV at the cleavage furrow [17]; SDV transformation agrees well with an earlier observed high membrane activity in dividing diatom cells [22, 23]. Furthermore, in plants a similar uptake mechanism for silicon has been observed [24]. We believe that macropinocytosis could account for the rapid uptake of external fluid to accommodate the need for sufficient silicon during valve formation, which has been called ‘surge uptake’ [10, 20], in particular when a larger vesicle transforms to the SDV and is compressed in the course of its alignment to the cleavage furrow.

Previous calculations on ‘classical’ pinocytosis have indicated that Si uptake and transport was not cost-effective for the cell in terms of bioenergetics, membrane recycling and kinetics [25]. The crux is that in macropinocytosis one larger vesicle is formed, which is in line with recent observations on the diatom *Thalassiosira pseudonana* [16] and observed presence of vacuolar-like structures with different functions [6].

The aim of the present study was to investigate which type of pinocytosis or other transport routes (including a SITs mediated one) play a role in Si uptake during initial and early valve formation. Silicic acid uptake measurements were combined with compartmental analysis (CA), a mathematical approach used to obtain information about the fate of a compound in a defined system [26, 27 and references therein]. CA has been used over decades for the description of tracer uptake kinetics in biology and chemistry, e.g. to describe the accumulation of technetium in plants [28] and the speciation of calcium in milk [29]. This approach consists of two parts: 1) experimental data on the overall behaviour of a compound in time and in the entire system (i.e. Si in the different parts of the diatom cell and the surrounding medium), and 2) the description of this whole system in a mathematical model. Based on physiological knowledge and/or the proposed transport route the studied system is divided into rationally defined compartments: i.e. the involved compound (in our case Si) is contained by different cellular parts (e.g. cytoplasm, SDV, etc.), or the involved compound exists in different chemical forms (i.e. dissolved silicic acid vs solid silica). Each compartment can have a different concentration of the compound under investigation (e.g. the Si concentration in the medium, in the cytoplasm, in the SDV, etc.). When the compound is taken up or transported from one compartment to another it passes a ‘barrier’ (e.g. regulation by a protein, a chemical reaction, etc.) which is described mathematically based on first order transport kinetics [26].

For each proposed uptake/transport route a mathematical model is composed describing the observed net uptake flux in time as a combination of all transport fluxes, which take place inside the system as a whole. The kinetic constants belonging to the different transport rates within the system are determined from the behaviour of the system over the entire time scale of the experiment. The experimental data (uptake/transport against time) determine the value of the involved kinetic constants. Because every system has a unique behaviour in time, depending on the transport processes that are taking place inside the system, it is possible to determine which mathematical model describes the system best [26].

The difference between CA and traditional uptake studies lies in the fact that in CA it is possible to get insight into transport processes of the whole system in time, while in traditional uptake studies only the overall net uptake is determined (often as uptake at a fixed point in time). In addition, the experimental time frames used in traditional uptake studies determines which processes are can be observed; some processes can proceed too fast (e.g. <seconds) or too slow (e.g. >hours) so that they are overlooked easily (i.e. the so called ‘hidden’ compartments in CA [26]). It is also possible that compartments containing very small amounts of the compound under study are too small to be distinguished [26]. The advantage of CA is the analysis of the whole system without the necessity to take every individual barrier between compartments into account, whereas the presence of ‘hidden’ compartments can be assessed. In addition CA allows analysis of distinct processes which occur in a specific stage of the cell cycle, in our case early diatom valve formation. Therewith, this approach differs from a previous study in which classical pinocytosis did not appear to be favorable [25].

Data on silicon uptake obtained in experiments with the radiotracer  $^{31}\text{Si}$ - $\text{Si}(\text{OH})_4$  [30] are used to calculate the transport rate constants in models describing the different Si uptake and transport mechanisms. By formulating and testing multiple models the one fitting best allows interpretation of the most likely process [26]. The short half life time of the radio-active tracer we used ( $t_{1/2}$   $^{31}\text{Si}$ =2.62 h) allows an experimental time frame that covers the rapid initial stages of valve formation [19, 31].

## 2 Materials and Methods

### 2.1 Chemicals for Radioactivity Studies

All chemicals used in this study were of analytical grade, obtained from Aldrich (Zwijndrecht, The Netherlands). All solutions were prepared in ultrapure Milli-Q grade water (18.2 M $\Omega$ /cm; Millipore, Billerica, MA, USA). For silicon

uptake the silicon isotope  $^{31}\text{Si}$  as silicic acid ( $t_{1/2}$ =2.62 h,  $\beta^-$  1.49 MeV) was produced in the nuclear reactor of the Reactor Institute Delft, Delft University of Technology, The Netherlands. No-carrier-added (i.e. without natural Si)  $^{31}\text{Si}$  (OH) $_4$  solution (specific activity 4.8 TBq/g) was prepared as described earlier [32], and was successfully used earlier in Si uptake studies in yeast [13].

### 2.2 Chemical Analyses of Medium and Cells

Inductively coupled plasma optical emission spectrometry (OES Optima 4300DV, Perkin Elmer, Boston, USA) was used to determine Si concentrations in the liquids. For calibration Merck CertiPUR standard solution 1703 (Amsterdam, The Netherlands) was used. Cells were directly removed from every sample by mild centrifugation (100 rpm, 10 min, Jouan CR4-11) and ICP-OES measurements were carried out immediately on the cell free supernatants. The  $^{31}\text{Si}$  activity (as  $\beta^-$  radiation) was measured on a LKB liquid scintillation counter (Tri-Carb 2750TR/LL, Packard, Meriden, USA) using liquid scintillation counting (LSC) cocktail (Ultima Gold XR<sup>TM</sup>, Perkin Elmer, Boston, USA).

### 2.3 Organisms and Culture Conditions

The experiments were carried out on the pennate diatoms *Pleurosira laevis* (FDCC L1451), *Navicula salinarum* (FDCC L1262), both from the Fresh Water Diatom Culture Collection Loras College, *Navicula pelliculosa* (CCMP 543), and the centric diatom *Coscinodiscus wailesii* (CCMP 2513), both from the Provasoli-Guillard National Centre for Culture of Marine Phytoplankton, Bigelow Laboratory for Ocean Sciences. The cells were exponentially grown in 500 mL batch cultures in 2 L Fernbach flasks using artificial seawater [33]. Permissive salinities, in practical salinity units (PSU), were applied: *P. laevis* 9 PSU, *N. salinarum* 20 PSU, and *N. pelliculosa* and *C. wailesii* both 33.7 PSU. Silicic acid concentrations under standard culture conditions were 400  $\mu\text{mol/L}$  for both *P. laevis* and *C. wailesii*, 200  $\mu\text{mol/L}$  for *N. salinarum*, and 100  $\mu\text{mol/L}$  for *N. pelliculosa*. Temperature (16  $^\circ\text{C}$ ) and light conditions ( $35 \pm 5$   $\mu\text{mol photons}\cdot\text{m}^{-2}\cdot\text{s}^{-1}$  under a 16:8 h day/night cycle) were constant during growth. The cells were incubated for at least 48 h in 250 ml Si-free medium in 1 L polycarbonate flasks (Nalgene) to induce synchronous valve formation when silicon is replenished [3, 19, 31, 34].

### 2.4 Analysis of Cellular Silicon

Silicon uptake studies in diatom cells were carried out by determination of  $^{31}\text{Si}$  uptake in the cells themselves instead of clearance of silicon from the medium. For  $^{31}\text{Si}$  uptake

analysis 0.1–0.5 ml freshly produced  $^{31}\text{Si}$  tracer solution was added to sterile growth medium and silicic acid stock solution in polypropylene tubes to a final volume of 0.5–1 mL. The solution was well mixed and allowed to equilibrate for at least 15 min at 16 °C prior to replenishing Si-synchronized cells with  $^{31}\text{Si}$ . To initiate synchronous valve formation 10–40 mL Si-depleted culture was brought into the culture tubes to establish different silicic acid concentrations. The kinetic parameters were determined at standard culture conditions for synchronously dividing cells. Additionally, these parameters were determined for synchronously dividing *P. laevis* cells, at medium concentrations of 3, 10, 20, 50, 100 and 200  $\mu\text{mol/L}$ . During the experiments the culture tubes were regularly mixed gently to ensure homogeneous culture conditions. Just prior to and following repletion of silicon, 500  $\mu\text{L}$  samples were taken at  $t=0, 2, 5, 10, 30, 60, 150, 240$  and 360 (not in all experiments) min. The chosen time frame, in view of the half life time of the tracer, allowed us to properly focus on the stages of early valve formation. Three subsamples for cell counting (1 mL), silicon determination (2–5 mL), and total  $^{31}\text{Si}$  (0.1–1 mL) were taken and immediately processed for further analysis; a laminar flow cabinet was used to prevent contamination by dust and to ensure sterile conditions during silicon replenishment and sampling. The cell density of *N. pelliculosa* and *N. salinarum* was determined by use of a Bürker Türk counting chamber. For *P. laevis* and *C. walesii* the cell density was determined by pipetting 10  $\mu\text{L}$  culture liquid on a microscope slide and counting all cells which were present. The other samples were filtered over a 0.45  $\mu\text{m}$  membrane filter (ME25, Whatman, Dessel, Germany, 25 mm diameter) and washed with 2.5 mL sterile medium, containing 5 mmol/L silicic acid. The activity of the  $^{31}\text{Si}$ -tracer of the sample (including the filter and cells) was determined. Prior to analysis, the sampled filters were dissolved in 10.0 mL LSC cocktail within a glass counting vial (20 mL). The volume of the liquid samples was adjusted to 5.0 ml with MilliQ grade water, mixed with 15.0 mL LSC cocktail and subsequently analyzed. In addition, 1.0 mL of the culture suspension was used for determining the total  $^{31}\text{Si}$ -tracer activity. The measured activity was corrected for silicic acid adsorption on the filter and related to the cell density and silicic acid concentration in the medium in order to determine the uptake of silicic acid per cell in  $\text{mol cell}^{-1}$ .

## 2.5 Mathematical Approaches

Compartmental analysis was performed with MicroMathScientist<sup>®</sup> software for time-resolved uptake of silicic acid in diatom cells. All uptake mechanisms are described in mathematical models (see Online Resource 2 for a detailed mathematical description of each model).

These models were fitted to the experimental data for silicon uptake over time using MicroMath Scientist<sup>®</sup> software and the residual sum of squares was determined. Also simulations were performed with this software. A statistical *F*-test was carried out on closely related models and the *P* value of this comparison was calculated; if  $P < 0.05$  the most complicated model was applied, whereas in other cases the simpler model was preferred. After fitting the models to experimental data followed by simulations, the models yielded values for transport rate constants ( $k_i$ ) between the different compartments and silicon contents ( $N_i$ ) in the distinct compartments involved. Note that the transport rate constants as determined by compartment analysis are valid for the entire time-span of the experiment, and discriminate for rates between compartments. As such they have a different unity (e.g.  $\text{L}/(\text{cell}\cdot\text{min})$  or  $\text{min}^{-1}$ ) in comparison to constants determined for uptake at a fixed point in time. It is possible to calculate the compartment volume ( $V_i$ ) that is required to reach a certain concentration ( $C_i$ ) in that compartment:

$$V_i = N_i/C_i \quad (1)$$

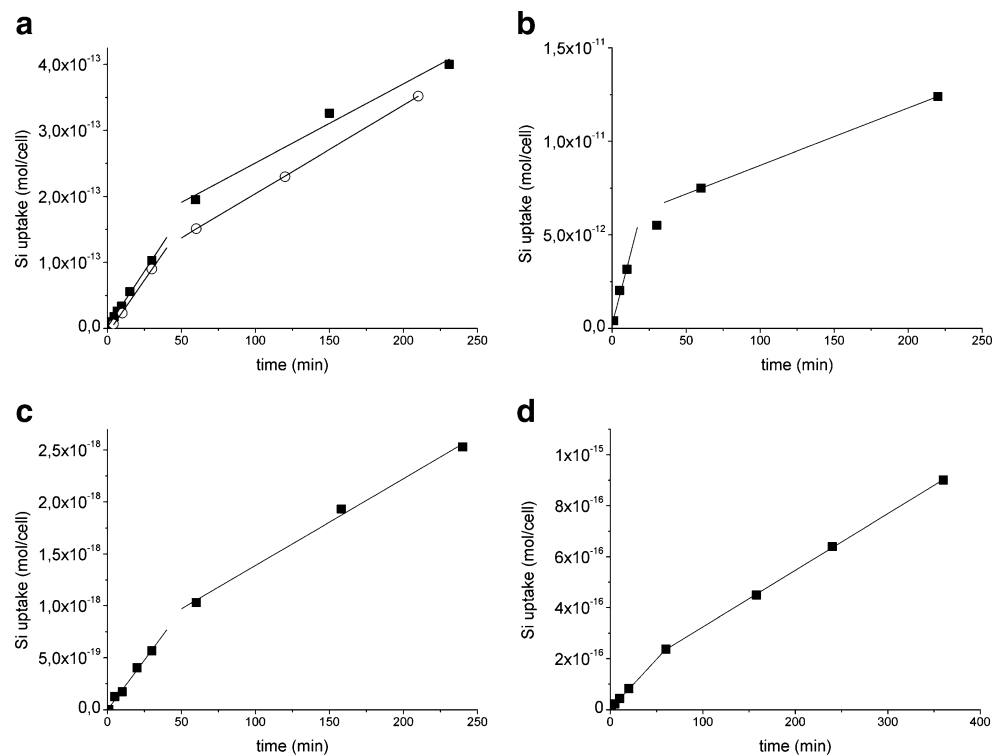
Using the volume of the entire cell the percentage of cell volume that is occupied by the compartment can be calculated.

## 3 Results

### 3.1 Silicic Acid Uptake and Mathematical Justification of Compartments Involved in Valve Formation

Silicic acid uptake (in  $\text{mol cell}^{-1}$ ) was determined during valve formation of *Coscinodiscus walesii*, *Navicula pelliculosa*, *N. salinarum* and *Pleurosira laevis*;  $^{31}\text{Si}$  was provided to silicon starved cells (Fig. 1). The uptake was examined over a fixed time frame (up to 6 h) for synchronously dividing cells. For *P. laevis* silicic acid uptake was determined at different replenishment concentrations (Fig. 1a). Emphasis was put on the rapid initial stage of valve formation. In every diatom species examined two distinct uptake rates could be identified. Si uptake was rapid in the first hour of valve formation; notice that the valve is completed in a 2-D dimension within about 2 h [19, 31]. This was followed by a steadily decreasing uptake rate in the following 4 h (Fig. 1). These distinct uptake rates confirm that more than one compartment in the cell is involved in the biosilicification process [26]. For every species the data obtained were used for the mathematical evaluation of the uptake mechanism in view of rationally defined models (Table 1). For *P. laevis* data of multiple uptake experiments were collected for different

**Fig. 1** Silicic acid uptake (in mol cell<sup>-1</sup>) under standard culture conditions by diatom cells following silicic acid addition to Si-limited cells for **a** *Pleurosira laevis* (■ 456 or ○ 21 μmol/L Si), **b** *Coscinodiscus wailesii* (456 μmol/L Si), **c** *Navicula pelliculosa* (140 μmol/L Si), and **d** *N. salinarum* (317 μmol/L Si). Two distinct uptake regimes can be recognized (*lines*)



silicic acid concentrations. It was determined that the diffusion of silicic acid from the culture medium through the water layer around the cell (the Nernst layer) into the cell itself was not rate limiting (see Online Resource 1). Consequently, this particular diffusion process formed no barrier and was excluded from the models.

Current knowledge of valve formation suggests that at least three cellular compartments should be sufficient to describe silicic acid uptake and transport for valve formation by means of SITs (Table 1, model F), which means that also three distinct uptake rates should be expected [26]. Three distinct uptake rates however were not identified in our silicic acid uptake patterns (Fig. 1). To assure that ‘hidden’ intermediate compartments were not

involved [26], we determined how many cell compartments could be discerned mathematically. For this the results of the uptake experiments for *P. laevis* were subjected to an extended analysis. Five models were formulated, each including a different number of cell compartments (Table 1, models A–E). These models were fitted mathematically (see also Online Resource 2) to the experimental data for Si uptake in order to assign the best fitting one. Next, the magnitude of the transport rate constants of this best fitting model was determined. Fitting the models to the results of six uptake experiments ([Si] ranging from 17 to 491 μmol/L) indicated that a model with just two cellular compartments plus the medium (model B) always resulted in the best fit ( $P < 0.05$ ).

**Table 1** The defined models based on current knowledge of the presence of distinctive compartments

model	compartments		remarks
	no.	description	
Models for determination of the number of compartments			
A	2	medium and cell	the cell is a black box
B	3	medium, 2 cell compartments	unidirectional flux to last compartment
C	4	medium, 3 cell compartments	unidirectional flux to last compartment
D	3	medium, 2 cell compartments	bidirectional flux to last compartment
E	4	medium, 3 cell compartments	bidirectional flux to last compartment
Models based on physiological knowledge and speculation			
F	4	medium, cytoplasm, SDV, silica	SIT-mediated transport
G	4	medium, tr. vesicles, SDV, silica	transport vesicle-mediated transport
H	3	medium, SDV, silica	macropinocytosis mediated transport



Although it was assumed that efflux from the final compartment (i.e. the solid silica inside the SDV) did not occur during rapid valve formation [6, 19, 31], such an efflux has been incorporated anyway to make the analysis complete (Table 1, models D and E). Model B (without efflux) from the final compartment appeared to outperform model D (including efflux). Moreover, there was no reverse flux from the final compartment in model D, because the value of the corresponding transport rate constant was (near) zero. Therefore, model B was assigned as the best performing one, so it can safely be concluded that optimally three compartments (medium and two cellular compartments) were involved in valve formation. Interestingly, this agreed with the observed two distinct uptake rates (Fig. 1).

The fact that only two uptake regimes seem to be operative does not give a conclusive answer as to the validity of the SITs-mediated uptake mechanism (3 cellular compartments; Table 1, model F). Since biological processes proceed relatively fast it may still be possible that one of the compartments was hidden in the experimental setup. This can be explained as follows: the compartment 1) reaches the state of equilibrium before the first measurement so its internal concentration of the target component does not alter during the experiment, 2) is very small compared to the others and for this reason cannot be distinguished, or 3) is not involved in the whole transport process at all [26]. To test the SIT mechanism by compartmental analysis it was of importance to determine whether or not hidden compartments occur. Because the saturation time is characteristic for each compartment, it can be used to assign any hidden compartment. The saturation time was calculated from the values of  $dN_x/dt$  and the maximal silicon contents of the compartments (See Online Resources 2 and 3). The characteristic saturation time ( $t_{char,sat}$ ) of all compartments involved displayed an order of magnitude of at least 100 min (Table 2), indicating that the silicic acid content in the applicable compartments was still changing during

valve formation and expectedly would be observed. Therewith, it was highly unlikely that the model for SITs-mediated uptake contained any hidden compartment so this mechanism indeed cannot explain the massive Si transport for silica deposition during valve formation and ‘surge’ uptake has been suggested instead [10, 11, 20]. However, alternative routes could be assessed.

### 3.2 Mathematical Assessment of Alternative Silicic Uptake Models

In view of the demand for high silicic acid concentrations during valve formation two mechanisms were selected for Si uptake and intracellular transport: 1) transport vesicle-mediated silicon uptake and transport towards the SDV involving 3 cellular compartments (Table 1, model G) and 2) macropinocytosis-mediated uptake from the medium with 2 cellular compartments of which the initially formed vesicle transforms to become the SDV (Table 1, model H). Since the model for transport vesicle-mediated silicon uptake contains three cellular compartments, this mechanism again infers action of a hidden compartment, matching with the observed dual uptake regime (Fig. 1). If so, an additional vesicle compartment should display very fast kinetics, making it literally hidden in the experimental setup (Table 2 and Online Resource 3). Mathematically, the algorithms for a transport vesicle-mediated mechanism only match with the model in which two cellular compartments are involved (Table 1, model B), with high saturation rates of transport vesicle compartment (see Online Resource 4). The production of large amounts of vesicles as needed for the fast saturation of the vesicle compartments in model G puts very high demands on the cell, and one could question whether this process is feasible for the organism. This is in line with earlier calculations [25] in spite of the fact that transport vesicles have been assigned in diatoms [1, 4, 23].

The results prompted us to further focus on macropinocytosis-mediated Si uptake (Table 1, model H).

**Table 2** Calculated magnitudes of minimum and maximum rates  $dN/dt$  (mol/(cell·min)) and  $dV_i/dt$  (L/(cell·min)) and characteristic saturation times for models F and G for *Pleurosira laevis*, see Online Resource 2 for equations

compartment	rate, eq. nr.	min–max value	char. saturation time (min)
Model F: SIT-mediated transport			
cytoplasm	$dN_c/dt$ , 2.19	$0-10^{-14}$	>100
SDV	$dN_s/dt$ , 2.20	$0-10^{-14}$	>100
valve	$dN_v/dt$ , 2.21	$0-10^{-14}$	>100
Model G: transport vesicle-mediated transport			
tr. vesicles	$dV_i/dt$ , 2.27	$10^{-11}-10^{-10}$	0.1–1
SDV	$dN_s/dt$ , 2.25	$0-10^{-14}$	>100
valve	$dN_v/dt$ , 2.26	$0-10^{-14}$	>100
Model H: macropinocytosis-mediated transport			
SDV	$dN_s/dt$ , 2.29	$0-10^{-14}$	>100
valve	$dN_v/dt$ , 2.30	$0-10^{-14}$	>100

If this mechanism is applicable, the larger vesicle formed intracellularly subsequently may be compressed towards the cleavage furrow by cellular and membrane activity [16, 17, 22, 23]; especially when simultaneously water is expelled [20, 35] the concentration of silicic acid to the threshold for autopolymerization would be achieved [14, 15]. For *T. pseudonana* it is demonstrated that silica is formed in the most compressed region of the SDV [16]. On the assumption that macropinocytosis plays a role in Si uptake, two distinct compartments within the SDV (i.e. solute and solid silica) should be involved; mathematically this notion matches the algorithms of model B (Table 1).

### 3.3 Kinetic Parameters of Macropinocytosis-Mediated Silicic Acid Uptake

Our study suggests that Si uptake during valve formation under standard culture conditions is described best by the macropinocytosis model (model H, Table 1). In order to determine its kinetic parameters and rate constants the model was fitted to experimental data for different Si concentrations in the medium (Fig. 2). The value of all transport rate constants decreased at Si concentrations above 200–300  $\mu\text{mol/L}$ , possibly as a result of a feedback mechanism, which implies that the diatom cell reached the

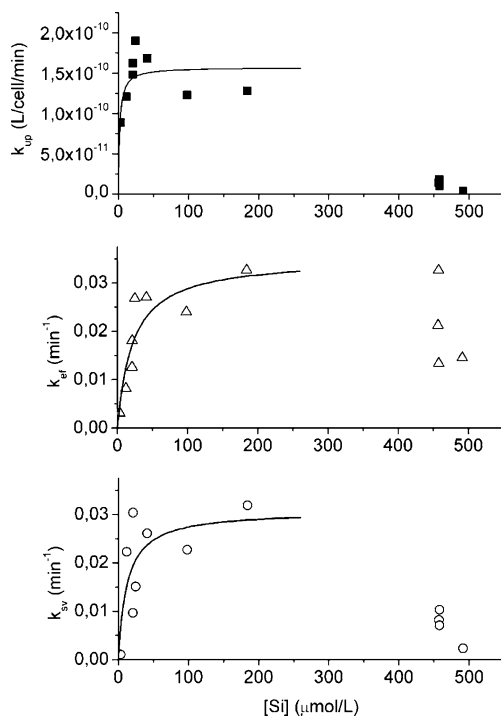


**Fig. 2** Calculated rate constants in *Pleurosira laevis* for different Si concentrations in the medium. ■ Si uptake from the medium ( $k_{\text{up}}$ ),  $\Delta$  Si efflux from cell ( $k_{\text{ef}}$ ), and  $\circ$  transformation of silicic acid to solid valve silica ( $k_{\text{sv}}$ ). Lines: Michaelis Menten kinetics in the range of 0–300  $\mu\text{mol/L}$  Si

optimal uptake rate and did not necessarily need to acquire more silicic acid.

As the rate constants are ruled by biological processes we evaluated whether a Michaelis Menten kinetics pattern could be observed for the values of these constants at different Si concentrations even for shorter experimental time frames [10 and various references therein]. The transport rate constants  $k_{\text{ef}}$  and  $k_{\text{sv}}$  obey Michaelis Menten kinetics at lower Si concentrations (0–300  $\mu\text{mol/L}$ , see lines in Fig. 2) in the medium. However, for Si uptake ( $k_{\text{up}}$ ) this was less obvious, although Michaelis Menten kinetics could be expected at lower Si concentrations (Table 3). This  $k_{\text{up}}$  also displayed a high affinity for silicic acid, and the  $K_{\text{m}}$  value (2.0  $\mu\text{mol/L}$ ) was correspondingly low. The rate constant for valve formation ( $k_{\text{sv}}$ ) revealed a much higher  $K_{\text{m}}$  value (12  $\mu\text{mol/L}$ ), whereas the  $K_{\text{m}}$  value of the efflux rate constant  $k_{\text{ef}}$  was even higher than any other rate constant (22  $\mu\text{mol/L}$ ). Using these rate constants the concentration of silicon species in the SDV ( $N_{\text{s}}$ ) and valve ( $N_{\text{v}}$ ) were calculated (Fig. 3, upper graph). This exercise showed that the silicic acid content in the SDV ( $N_{\text{s}}$ ) reached a maximal value between 1 and 2 h, in line with the rapid valve formation determined earlier by fluorescent probing [19, 31]. This maximal value (Fig. 3, lower graph) depended on the silicic acid concentration in the medium and appeared to increase from zero to maximal values in the range of  $3.2 \cdot 10^{-13}$  mol/cell at a medium concentration of 200–300  $\mu\text{mol/L}$  Si. At higher medium concentrations

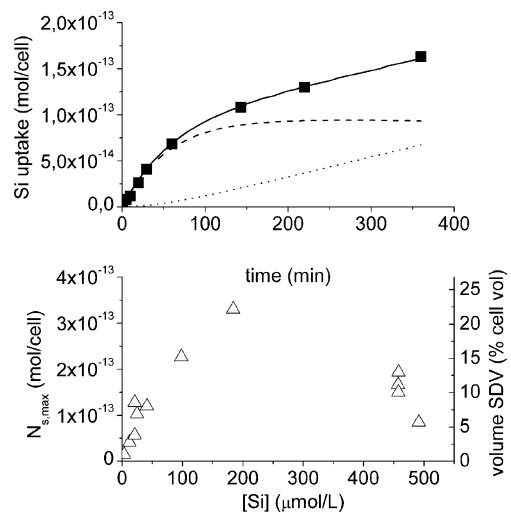


**Fig. 3** Upper graph: ■ typical result obtained by fitting total silicic acid uptake per cell to model H and by simulation with the rate constants *Pleurosira laevis* (490  $\mu\text{mol/L}$  Si). Straight line: fitted total Si in cell, dashed line: Si in SDV, dotted line: Si deposited in the valve. For all datasets similar results were obtained. Lower graph: the calculated maximal maximum amount of Si in the SDV in *Pleurosira laevis* (value  $N_{\text{s}}$ ), depending on Si concentration in the medium. For all these data points ( $\Delta$ ) the cell volume occupied by the SDV (in % as indicated on the Y-axis at the right) was calculated for Si concentrations inside the SDV at 2 mmol/L

**Table 3** Michaelis-Menten constants of the rate constants in macropinocytosis mediated silicic acid uptake (model H) for *Pleurosira laevis*

rate constant	transport process	Michaelis-Menten constants	
		$K_m$ ( $\mu\text{mol/L}$ )	$k_{\text{max}}$
$k_{\text{up}}$	medium to SDV	$2.0 \pm 1.7$	$1.6 \pm 0.16 \cdot 10^{-10} \text{ L} \cdot (\text{cell} \cdot \text{min})^{-1}$
$k_{\text{ef}}$	efflux to medium	$22 \pm 10$	$3.5 \pm 0.57 \cdot 10^{-2} \text{ min}^{-1}$
$k_{\text{sv}}$	SDV to valve	$12 \pm 11$	$3.1 \pm 0.73 \cdot 10^{-2} \text{ min}^{-1}$

the maximal  $N_s$  decreased, in agreement with the decrease in the rate constant values (Fig. 2).

We also investigated whether the amount of silicic acid in the SDV ( $N_s$ ) was sufficient ( $>2 \text{ mmol/L}$  [14, 15]) to initiate silica polymerization by calculation of the SDV volume correlating with this concentration. With this information the percentage of cell volume occupied by the SDV could then be estimated (Fig. 3, lower graph). The SDV volume which is required to maintain the Si concentration at  $2 \text{ mmol/L}$  reached from 1% of the cell volume ( $3.5 \mu\text{mol/L}$  Si in the medium) to 22% ( $200 \mu\text{mol/L}$  Si in the medium). Apparently, the calculated Si concentrations of the SDV and its volume dependency for silica deposition yielded plausible conditions to achieve valve formation in *P. laevis*. To confirm whether the approach tested in *P. laevis* applied to the other species too, we conducted the same compartmental analysis for *C. wailesii*, *N. pelliculosa*, and *N. salinarum*, using the experimental data on silicic acid uptake (Fig. 1). After assessment of the number of cell compartments involved in Si uptake during valve formation of these other species it appeared that the model comprised of two cellular compartments (Table 1, models B and H) unambiguously was best fitting. As in *P. laevis*, the rate constants involved ( $k_{\text{up}}$ ,  $k_{\text{ef}}$  and  $k_{\text{sv}}$ ), the maximal Si content in the SDV ( $N_s$ ), and the volume of the SDV were calculated (Table 4). The rate constants for efflux ( $k_{\text{ef}}$ ) and transport to the valve ( $k_{\text{sv}}$ ) were in the same order of magnitude as was observed in *P. laevis*. The SDV volume varied between species: it occupied 6.1–12% of the cell volume (i.e. at  $[\text{Si}]$  inside the SDV is  $2 \text{ mmol/L}$ ). These percentages demonstrate that silica polymerization and valve formation may well proceed by the way we suggest here. Altogether, the macropinocytosis-mediated uptake of silicic acid for valve formation proved to be the best match in terms of cell physiology, in particular when soluble silicic acid inside this vesicle, potentially the initial SDV, concentrates towards saturation levels during compression and 2-D orientation upon maturation.

#### 4 Discussion and Conclusions

Compartmental analysis has so far never been undertaken in studies of the uptake kinetics of silicic acid during diatom valve formation. This combined experimental-mathematical

approach to examine all relevant options for Si-uptake (Table 1) has allowed us to assess the number of compartments involved in order to define the model that fitted the experimental data best. Our results reveal that during valve formation uptake mechanisms with just two cellular compartments optimally matched the experimentally determined uptake rates instead of any other mechanism that required additional cellular compartments. SITs surely do play a role in diatoms [10, 11, 36–39], but SIT-mediated Si uptake and transport could not be assigned as the major process in early valve formation. The SITs-mediated uptake that has been proposed [10, 11] would require intracellular transport and stabilization and thus involvement of an additional cellular compartment. SIT protein expression varies little during valve formation [37, 38] so it seems unlikely that only SITs take part in the first 1–2 h when the 2-D valve structure is deposited [19, 31].

According to our models (Table 1) two mechanisms for Si uptake during valve formation remain. One is pinocytosis in which rapidly saturating transport vesicles play a role, but the fast production of high amounts of small vesicles puts a high demand on the cell, which makes this mechanism questionable under these circumstances [25]. In previous work it was proposed that smaller earlier identified intracellular transport vesicles [1, 2, 4] just may deliver the organic compounds that are involved in the valve formation process [7]. The other mechanism describes macropinocytosis-mediated Si uptake and subsequent transformation of the compartment and its liquid content to become the SDV in which solid biosilica forms. This well matches recent observations in diatoms, revealing presence of a larger flattened vesicle in which biosilicification occurs at the most compressed site while actin filaments mold and/or appress the SDV at the site of the cleavage furrow [16, 17]; SDV molding processes and elevated membrane activity indeed have been described earlier to occur during diatom cell division [1, 4, 22, 23]. The model for macropinocytosis-mediated Si uptake clearly outperformed the others, matched our experimental data best, and accounted for uptake of sufficient silicic acid to produce the initial nanostructured 2-D base of the new hypovalve. In fact, this pathway for processing extracellular fluid agrees well with observations of nanostructural changes in diatom biosilica that are induced by external ionic strength [7].



**Table 4** Rate constants and other parameters for *Navicula pelliculosa*, *N. salinarum* and *Coscinodiscus wailesii* describing Si uptake by macropinocytosis (model H) under standard culture conditions

Organism		<i>N. pelliculosa</i>	<i>N. salinarum</i>	<i>C. wailesii</i>
cell volume	L/cell	$7.86 \cdot 10^{-15}$	$1.37 \cdot 10^{-12}$	$2.40 \cdot 10^{-8}$
[Si] medium	$\mu\text{mol/L}$	140	317	456
$k_{\text{up}}$	$\text{L} \cdot (\text{cell} \cdot \text{min})^{-1}$	$2.53 \cdot 10^{-16}$	$2.66 \cdot 10^{-14}$	$9.42 \cdot 10^{-10}$
$k_{\text{ef}}$	$\text{min}^{-1}$	0.00739	0.0188	0.0656
$k_{\text{sv}}$	$\text{min}^{-1}$	0.00813	0.0253	0.00565
$N_{\text{s,max}}$	mol/cell	$1.58 \cdot 10^{-18}$	$1.66 \cdot 10^{-16}$	$5.76 \cdot 10^{-12}$
vol SDV (2 mmol/L Si)	% cell vol.	10.0	6.05	12.0

Our analysis suggests that the SDV volume is of importance in view of the increasing internal silicic acid concentration (Fig. 3, lower graph and Table 4) and most probably the solid silica formed is also adjusted or molded in shape by cellular activity during the 2-D development of the new hypovalve. The calculated SDV volumes to enable silica polymerization to form the new hypovalve are as expected; they agree well with the observed pale fluorescent vesicles that are observed in studying valve morphogenesis [19, 31, 40]. If simultaneously water is expelled [20, 35] the SDV constituents concentrate, allowing silicic acid to polymerize when the proper saturation level has been reached [14, 15]. This concentration is supported by the intensity change of the compound used in fluorescent probing [40] while at the same time the shape of the SDV, and potentially its volume, changes upon compression towards the cleavage furrow [16, 17, 19, 31]. It should also be noted that the saturation level not only depends on the presence of other ions and surfactants, but on their concentrations as well. Both steer the polymerization reaction [14, 15] and account for the salinity effect on the nanostructure of the biosilica [7].

The values of the observed uptake rate constants for Si uptake and transport inside the cell decrease at Si concentrations exceeding  $300 \mu\text{mol/L}$  (Fig. 2). It is possible that diatom possess some sensory or feedback mechanisms to control the Si concentration in the cell. Although this has to be further investigated, it has been shown that a Si sensory system is involved in regulation of diatom DNA transcription [42]. The transport rate constants could well obey Michaelis-Menten kinetics (Fig. 2, Table 2) for lower Si concentrations, in agreement with previous observations [10 and many references therein, 41]. The affinities for the Si uptake on the one hand and intracellular transport on the other clearly differed, which is seen in the  $K_m$  values of the rate constants. The high affinity for silicic acid of the uptake process—related to the cell's absolute need for silicic acid—is displayed in the low  $K_m$  value of the rate constant  $k_{\text{up}}$  ( $2.0 \pm 1.7 \mu\text{mol/L}$  Si; Table 3) and should enable the cell to take up silicic acid very efficiently. The  $K_m$  value of silicic acid transformation inside the SDV to

solid silica of the valve ( $k_{\text{sv}}$ ) was clearly higher ( $12 \pm 11 \mu\text{mol/L}$  Si), suggesting a threshold value to initiate valve formation. In this respect one should notice that indeed a threshold of silicic acid controls the expression of DNA polymerase in diatoms [42]. It is important to find out whether these transcription and valve formation thresholds have a concerted mode of action to assure that cell division only proceeds when sufficient silicon is available. The  $K_m$  value for Si efflux from the SDV ( $k_{\text{ef}}$ ) was higher than the other rate constants ( $22 \pm 10 \mu\text{mol/L}$ ) to ensure that Si is not removed from the cell under Si starvation; this agrees with earlier observations [43]. At a cellular level, efflux should be considered a feedback mechanism to remove the surplus of Si in the cell.

Macropinocytosis enables the fast Si uptake which has been referred to as surge uptake [10, 11] and is in line with the high Si demand when new hypovalves are formed. This pathway surely would be a simple cost-effective mechanism to efficiently contain and concentrate silicic acid at the proper location. The advantage is that intracellular transport and/or stabilization, also to prevent unwanted autopolymerization, is not required with macropinocytosis-mediated Si uptake. Our simulations indicate that for valve formation the macropinocytosis pathway does not cause drawbacks related to the SDV volume, which is different in a simulation based on classical pinocytosis in which multiple smaller vesicles are involved [25].

We conclude that in diatoms separate pathways exist for Si uptake and transport, and one of these serves the rapid uptake of larger amounts needed for valve formation [20]. Other ones would then be responsible for Si uptake/transport for different silicification processes such as formation of the girdle band(s) or specific protrusions [1, 4]. The presence of Si inside cytoplasm and organelles (e.g. mitochondria, microsomes, chloroplasts) as well as its role in controlling DNA replication indicates that Si is present constitutively [5, 42]. SIT protein expression is quite constant in the course of girdle band and valve formation, in spite of the fact that mRNA levels increase during girdle band formation [36]. These transporters are not considered to be solely involved in massive silicon uptake at high silicon demand [10], as could be expected

at major biosilicification events such as valve formation. In line with previous observations [10, 11], SITs-mediated silicon transport would account for Si uptake at low concentrations and/or small quantities, making it tempting to suggest that SITs are used to control intracellular Si concentrations at locations other than the SDV. In contrast, macropinocytosis could largely account for Si uptake during valve formation, but in a different form than diffusion mechanisms in surge uptake. Further research on the different components of the molecular machinery involved is necessary to see whether these are specifically activated and controlled prior to, during and following valve formation. In fact, the genes potentially involved in macropinocytosis are assigned in the diatom genome [39], whereas cytoskeleton proteins such as actin [17] are intimately associated with valve morphogenesis.

**Acknowledgements** We thank Jorrit Heikamp and Tona Verburg (Department of Radiation, Radionuclides & Reactors, Section Radiation and Isotopes for Health, Delft University of Technology) for assistance in respectively silicon uptake experiments and mathematics and modeling in the compartmental analysis.

**Open Access** This article is distributed under the terms of the Creative Commons Attribution Noncommercial License which permits any noncommercial use, distribution, and reproduction in any medium, provided the original author(s) and source are credited.

## References

- Pickett-Heaps JD, Schmid AMM, Edgar LA (1990) The cell biology of diatom valve formation. *Prog Phycol Res* 7:1–168
- Round FE, Crawford FM, Mann DG (1990) *Diatoms: the biology and morphology of the genera*. Cambridge Univ Press, Cambridge
- Coombs J, Volcani BE (1968) Studies on the biochemistry and fine structure of silica-shell formation in diatoms. Chemical changes in the wall of *Navicula pelliculosa* during its formation. *Planta* 82:280–292
- Gordon R, Drum RW (1994) The chemical basis of diatom morphogenesis. *Int Rev Cytol* 150:243–272
- Mehard CW, Sullivan CW, Azam F, Volcani BE (1974) Role of silicon in diatom metabolism. 4. Subcellular localization of silicon and germanium in *Nitzschia alba* and *Cylindrotheca fusiformis*. *Physiol Plant* 30:265–272
- Vrieling EG, Gieskes WWC, Beelen TPM (1999) Silicon deposition in diatoms: control by the pH inside the silicon deposition vesicle. *J Phycol* 35:548–559
- Vrieling EG, Sun Q, Tian M, Kooyman PJ, Gieskes WWC, van Santen RA, Sommerdijk NAJM (2007) Salinity-dependant diatom biosilicification implies an important role of external ionic strength. *Proc Natl Acad Sci USA* 104:10441–10446
- Lopez PJ, Desclès J, Allen AE, Bowler C (2005) Prospects in diatom research. *Curr Opin Biotechnol* 16:180–186
- Wong Po Foo C, Huang J, Kaplan DL (2004) Lessons from seashells: silica mineralization via protein templating. *Trends Biotechnol* 22:577–585
- Thamatrakoln K, Hildebrand M (2008) Silicon uptake in diatoms revisited: a model for saturable and nonsaturable uptake kinetics and the role of silicon transporters. *Plant Physiol* 146:1397–1407
- Hildebrand M (2008) Diatoms, biomineralization processes, and genomics. *Chem Rev* 108:4855–4874
- Johnson RN, Volcani BE (1977) The uptake of silicic acid by rat liver mitochondria. *Biochem J* 172:557–568
- Brasser HJ, Krijger GC, Wolterbeek HT (2008) On the beneficial role of silicon to organisms: a case study on the importance of silicon chemistry to metal accumulation in yeast. *Biol Trace Elem Res* 125:81–95
- Iler RK (1979) *The Chemistry of Silica*. John Wiley & Sons, New York
- Brinker CJ, Scherer GW (1990) *Sol–Gel Science*. Academic Press, New York
- Hildebrand M, Kim S, Shi D, Scott K, Subramaniam S (2009) 3D imaging of diatoms with ion-abrasion scanning electron microscopy. *J Struct Biol* 166:316–328
- Tesson B, Hildebrand M (2010) Dynamics of silica cell wall morphogenesis in the diatom *Cyclotella cryptica*: substructure formation and the role of microfilaments. *J Struct Biol* 169:62–74
- Gröger C, Sumper M, Brunner E (2008) Silicon uptake and metabolism of the marine diatom *Thalassiosira pseudodana*: solid-state Si-29 NMR and fluorescence microscopic studies. *J Struct Biol* 161:55–63
- Heredia A, van der Strate HJ, Delgadillo I, Basiuk VA, Vrieling EG (2008) Analysis of organo-silica interactions during valve formation in synchronously growing cells of the diatom *Navicula pelliculosa*. *Chembiochem* 9:573–584
- Gordon R, Losic D, Tiffany MA, Nagy S, Sterrenburg FAS (2008) The glass menagerie: diatoms for novel applications in nanotechnology. *Trends Biotechnol* 27:116–127
- Rogerson A, deFreitas ASW, McInnes AG (1987) Cytoplasmic silicon in the centric diatom *Thalassiosira pseudonana* localized by electron spectroscopic imaging. *Can J Microbiol* 33:128–131
- Kühn S, Brownlee C (2005) Membrane organisation and dynamics in the marine diatom *Coscinodiscus wailesii* (Bacillariophyceae). *Bot Mar* 48:297–305
- Schmid AMM (1986) Wall morphogenesis in *Coscinodiscus wailesii* Gran et Angst II: cytoplasmic events of wall morphogenesis. In: Richard M (ed) *Proceedings of the 8th International Diatom Symposium*. Koeltz, Königstein, pp 293–314
- Neumann D, De Figueirido C (2002) A novel mechanism of silicon uptake. *Protoplasma* 220:59–67
- Thamatrakoln K, Kusta AB (2009) When to say: can excessive drinking explain silicon uptake in diatoms? *Bioessays* 31:322–327
- Shipley RA, Clark RE (1972) *Tracer Methods for in vivo Kinetics—Theory and Applications*. Academic Press, New York
- Brown RF (1980) Compartmental system analysis: state of the art. *IEEE Trans Biomed Eng* 27:1–11
- Krijger GC, Harms AV, Leen R, Verburg TG, Wolterbeek B (1999) Chemical forms of technetium in tomato plants;  $TcO_4^-$ , Tc-cysteine, Tc-glutathione and Tc-proteins. *Environ Exp Bot* 42:69–81
- Kolar ZI, Verburg TG, van Dijk HJM (2002) Three kinetically different inorganic phosphate entities in bovine casein micelles revealed by isotopic exchange method and compartmental analysis. *J Inorg Biochem* 90:61–66
- Firestone BR, Shirley VS (1996) *Table of Isotopes*, 8th edn. John Wiley & Sons, New York
- Hazelaar S, van der Strate HJ, Gieskes WWC, Vrieling EG (2005) Monitoring rapid valve formation in the pennate diatom species *Navicula salinarum* (Bacillariophyceae). *J Phycol* 41:354–358
- Brasser HJ, Gürboğa G, Kroon JJ, Kolar ZI, Wolterbeek HT, Volkens KJ, Krijger GC (2006) Preparation of  $^{31}Si$ -labelled silicate: a radiotracer for silicon studies in biosystems. *J Label Compd Radiopharm* 47:867–882
- Veldhuis MJW, Admiraal W (1987) Influence of phosphate-depletion on the growth and colony formation of *Phaeocystis pouchetii*. *Mar Biol* 95:47–54

34. Hazelaar S (2006) Nanoscale architecture; the role of proteins in diatom silicon biomineralization. PhD Thesis, University of Groningen, The Netherlands. <http://irs.uib.rug.nl/ppn/296120626>
35. Grachev MA, Annenkov VV, Likhoshway YV (2008) Silicon nanotechnologies of pigmented heterokonts. *Bioessays* 30:328–337
36. Hildebrand M, Volcani BE, Gassmann W, Schroeder JI (1997) A gene family of silicon transporters. *Nature* 385:688–689
37. Thamtrakoln K, Hildebrand M (2007) Analysis of *Thalassiosira pseudonana* silicon transporters indicates distinct regulatory levels and transport activity through the cell cycle. *Euk Cell* 6:271–279
38. Thamtrakoln K, Alverson AJ, Hildebrand M (2006) Comparative sequence analysis of diatom silicon transporters: toward a mechanistic model of silicon transport. *J Phycol* 42:822–834
39. Armbrust EV, Berges JA, Bowler C, Green BR, Martinez D, Putnam NH, Zhou SG, Allen AE, Apt KE, Bechner M et al (2004) The genome of the diatom *Thalassiosira pseudonana*: ecology, evolution, and metabolism. *Science* 306:79–86
40. Shimizu K, Del Amo Y, Brzezinski MA, Stucky GD, Morse DE (2001) A novel fluorescent silica tracer for biological silicification studies. *Chem Biol* 8:1051–1060
41. Martin-Jézéquel V, Hildebrand M, Brzezinski MA (2000) Silicon metabolism in diatoms: implications for growth. *J Phycol* 36:821–840
42. Okita TW, Volcani BE (1977) The deoxyribonucleic acid polymerases from the diatom *Cylindrotheca fusiformis*. Partial purification and characterization of four distinct activities. *Biochem J* 167:601–610
43. Sullivan CW (1976) Diatom moneralization of silicic acid. 1. Si (OH)<sub>4</sub> transport characteristics in *Navicula pelliculosa*. *J Phycol* 12:390–396